



OPEN ACCESS

EDITED BY

Alessandro Ruggiero,
University of Salerno, Italy

REVIEWED BY

Slavica Miladinovic,
University of Kragujevac, Serbia
Mladen Radojković,
University of Priština in Kosovska Mitrovica,
Serbia

*CORRESPONDENCE

Tomoko Hirayama,
✉ tomoko@me.kyoto-u.ac.jp

RECEIVED 21 April 2024

ACCEPTED 18 June 2024

PUBLISHED 15 July 2024

CITATION

Chun H, Hirayama T, Yamashita N, Hatano N,
Tatsumi K and Kuriyama R (2024), Shear
properties and dynamic responses of greases in
a micrometer-order gap.
Front. Mech. Eng 10:1420852.
doi: 10.3389/fmech.2024.1420852

COPYRIGHT

© 2024 Chun, Hirayama, Yamashita, Hatano,
Tatsumi and Kuriyama. This is an open-access
article distributed under the terms of the
[Creative Commons Attribution License \(CC BY\)](https://creativecommons.org/licenses/by/4.0/).
The use, distribution or reproduction in other
forums is permitted, provided the original
author(s) and the copyright owner(s) are
credited and that the original publication in this
journal is cited, in accordance with accepted
academic practice. No use, distribution or
reproduction is permitted which does not
comply with these terms.

Shear properties and dynamic responses of greases in a micrometer-order gap

Hanul Chun¹, Tomoko Hirayama^{1*}, Naoki Yamashita²,
Naoya Hatano¹, Kazuya Tatsumi^{1,2} and Reiko Kuriyama¹

¹Graduate School of Engineering, Department of Mechanical Engineering and Science, Kyoto University, Kyoto, Japan, ²Department of Mechanical Engineering and Physics, Kyoto Institute of Technology, Kyoto, Japan

Grease is used as a lubricant in a wide range of fields, including bearings, because it reduces friction, prevents harmful wear of components, protects against rust and corrosion, and acts as a seal to prevent the invasion of dirt and water. Although most of the research on grease has focused on the environment inside the bearing, there has been little research on the fundamental lubrication mechanism of grease. It is known that thickeners, which keep a complex three-dimensional structure in the grease, have a significant effect on the shear characteristics of grease, and it is assumed that this is due to the orientation of the thickener structure in the shear direction. In this study, the apparent viscosity of grease in a micro-order gap was measured using our original viscometer and compared with the apparent viscosity measured with a submillimeter-order gap rheometer because grease may show different rheological properties compared to conventional measurements. In addition, the dynamic response of viscous resistance that appeared when each grease was subjected to a change in the shear force was quantitatively evaluated using relaxation time. As a result, the apparent viscosity remarkably decreased in a micro-order gap compared to a submillimeter gap, and two types of shear thinning mechanisms were proposed based on the orientation of the thickener: one caused by the narrow gap and the other by the shear force. In addition, the behavior of viscous resistance due to changes in the shear force depended on the type of thickener. It was also confirmed that the relaxation time of each grease correlates with its oil film-forming ability and the entanglement level of the thickener's structure. Furthermore, the mechanism of the dynamic response was proposed based on the reorientation of thickeners.

KEYWORDS

grease, micrometer gap, apparent viscosity, thickener structure, orientation

1 Introduction

Tribology is one of the academic disciplines in the field of mechanical engineering that studies phenomena and properties related to friction, wear, and lubrication on sliding surfaces, which play an important role in industry and daily life. Understanding the properties of friction and lubrication between sliding surfaces and ensuring their sliding operation with a lower friction coefficient under optimal conditions is critical to improving the efficiency and reliability of mechanical components, resulting in these tribological studies extending the life of machines and reducing maintenance costs even while considering (Bhushan and Ko, 2003; Kandeva et al., 2016; Woydt, 2021; Bukvić et al., 2024).

In the recent trend toward further energy conservation in machinery and equipment, demand for lubricating grease is increasing even more (Akhtar et al., 2016; Gohar and Rahnejat, 2018; Rawat and Harsha, 2019). With the recent trend toward electric vehicles (EVs) in automobiles, there is a stronger need than ever before to reduce friction to meet the growing demand for rolling bearings, and the development of lubricating grease that can achieve lower friction has been recognized as one of the keys to this trend. Compared to lubricating oil, grease has a longer replenishment interval and is less prone to leakage and dispersal (Lugt, 2009; Farfan-Cabrera, 2019; Shah et al., 2021).

Grease is widely used as a lubricant for rolling bearings (Lugt, 2009), and studies have been conducted on the behavior of grease in bearing operation, bearing operating life (Lugt et al., 2023), and frictional resistance (Cousseau et al., 2011) from the viewpoint of grease lubrication. There are churning and channeling, which describe the macroscopic grease lubrication condition in the bearing. On one hand, the churning state is when the grease that has been churned up by the rolling elements flows back into the raceway and is churned up again by the rolling elements (Lugt, 2009). Channeling, on the other hand, is a state in which the grease is kept stirred up by the rolling elements, the amount of grease flowing in the bearing becomes small, and the viscous resistance caused by the grease goes low, making it a preferred lubrication state (Chatra et al., 2020). Numerous studies have been reported for the two states, churning and channeling, in grease lubrication or for the transition process to both states (Cann and Lubrecht, 1999; Cann et al., 2001; Cann, 2007; Lugt, 2009; Gao et al., 2018; Chatra et al., 2020; Chatra et al., 2021; Chatra K R et al., 2022; Obata et al., 2024; Shetty et al., 2024). With the recent development of observation technology, it has become possible to observe the lubrication state inside bearings using X-rays and neutron beams (Noda et al., 2020; Sakai et al., 2021). In addition, various studies have been conducted to analyze and predict the mechanism of grease lubrication in rolling bearings and the film thickness under elastohydrodynamic (EHL) contact (Cann and Lubrecht, 1999; Cann, 2007; Cen and Lugt, 2019; Wu et al., 2022) since rolling bearings are the main application of grease (Cann et al., 2001; Lugt, 2009; Cen and Lugt, 2019; Chatra et al., 2020). However, not many fundamental studies have attempted to elucidate the basic lubrication mechanism of grease away from the concept that is used in rolling bearings (Mansot et al., 1989; Chapkov et al., 2007; Saatchi et al., 2017; Camousseigt et al., 2023).

Typical greases consist of thickener fibers with a three-dimensional structure and base oil (Lugt, 2016). The first consideration in the use of grease on mechanical sliding surfaces is its rheological properties. The relationship between thickeners and grease lubrication properties has been reported. Suetsugu et al. (2013) elucidated that the network density of the thickener in grease is related to its storage modulus. Delgado et al. investigated how the microstructure of the lithium complex soap impacts the tribological properties of greases, the effect of cooling rate during grease production on fiber length and flexibility, and how thickener size influences the structural and fiber strength of thickeners. They also examined the relationship between local viscoelastic properties and thickener structure at the submicron scale, finding that viscosity increased with higher thickener

concentrations. Still, the thickness, length, and structural stiffness of the thickener fibers remained constant (Delgado et al., 2005). There is also a precedent for using FE-SEM, FT-IR, and XPS to investigate how the microstructure of the thickener affects the rheological and tribological properties of the grease (Onoda et al., 2021). In addition, the relationship between thickener structure and its shear strength was studied by changing the shear rate in lithium and urea greases, and the effect of thickener chemical structure on grease oil film formation has been studied (Mubashshir and Shaikat, 2019).

However, the specific correlation between the microstructure of the thickener and the rheological property of the grease is still unclear. Hotten proposed a model in which the thickener structure in the grease is oriented or broken down at a high shear rate. Still, the oriented thickener structure partially returns to its original structure when the sliding operation stops and returns to a static state (Hotten, 1955). Moreover, several other theoretical models have been proposed in the past, but they have not yet been established as useful models for actual grease lubrication analysis (Bristeau et al., 1980; Abdali et al., 1992; Radulescu et al., 2003). Furthermore, most studies on grease have been limited to ball bearings, the main application of grease (Hutton, 1975; Cann and Lubrecht, 1999; Cann, 2007; Lugt, 2009; Cousseau et al., 2011; Maksimova et al., 2018; Cen and Lugt, 2019; Hirayama et al., 2020; Noda et al., 2020; Chatra et al., 2021; Sakai et al., 2021; Lugt et al., 2023), and few fundamental studies have focused on the underlying fundamental lubrication mechanisms and properties of grease under shear.

Originally, it is well known that grease shows viscosity reduction characteristics in response to the shear rate. Generally, parallel plate or cone plate viscometers are used to obtain the viscosity characteristics of grease in response to the shear rate. However, in tribological situations, the gap between two sliding surfaces is on the order of the nanometer to the micrometer at most, which is much narrower than the gap realized by such typical viscometers. Considering this, the shear properties of oil films containing oiliness additives in micrometer gaps were investigated. It has been proposed that the absolute size of the gap, not the shear rate, determines whether interfacial sliding occurs, and it has been reported that the shear force decreases as the gap narrows (Hirayama et al., 2020). On the other hand, until now, no studies have evaluated grease properties in few-micron gaps, and the behavior of the grease in gaps narrower than thickener fibers has remained unknown. Since the lubrication environment is expected to become more severe with the miniaturization of future machine elements, research on grease in micrometer gaps is essential.

In this study, the parallel disk viscometer developed in the previous study (Hirayama et al., 2020) was used to investigate the shear characteristics of grease in a micrometer gap. First, the sliding gap was estimated using the base oil to measure the gap length by the vertical load. The apparent viscosity of the grease was then measured according to various gaps in micrometer order and compared to the apparent viscosity measured by a conventional viscometer with a submillimeter gap. In addition, the response force of the grease sandwiched in the micrometer gap to step changes in the shear rate as the input was investigated, and its dynamic viscosity characteristic behavior was finally discussed.

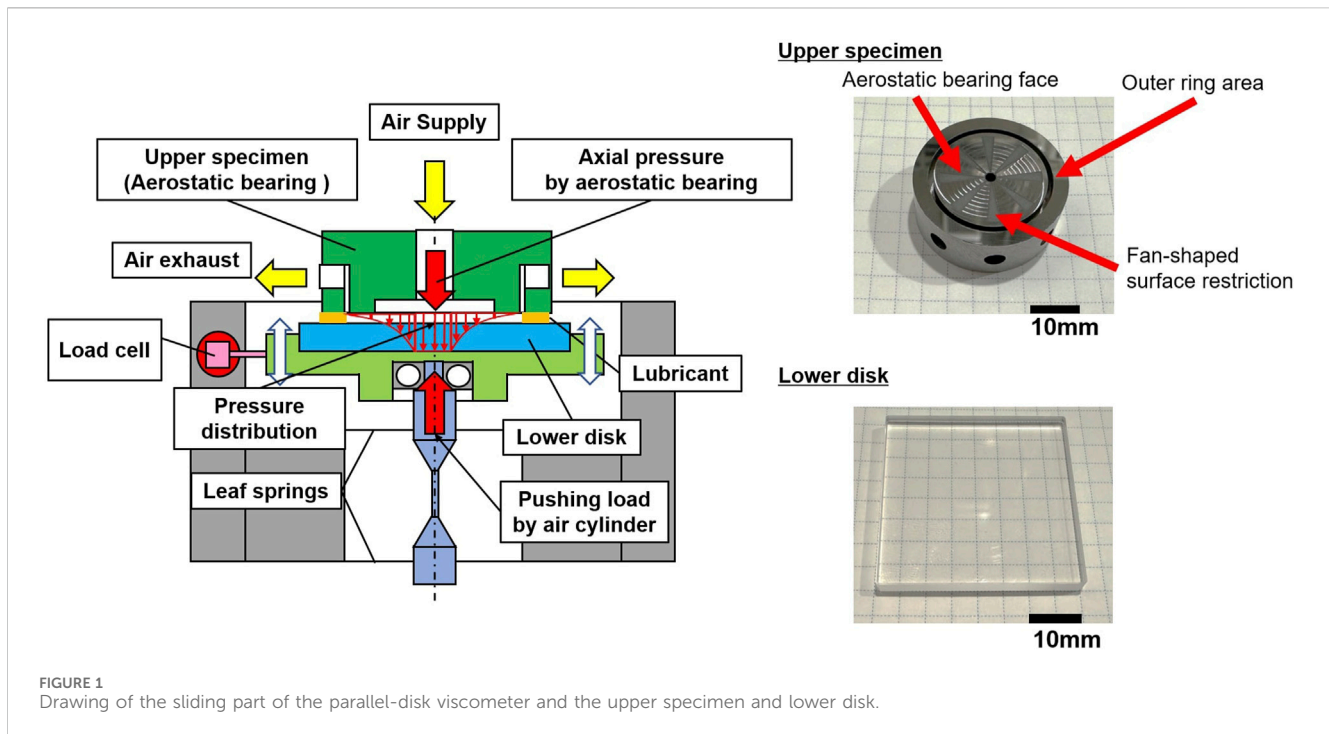


FIGURE 1 Drawing of the sliding part of the parallel-disk viscometer and the upper specimen and lower disk.

2 Parallel-disk viscometer

2.1 Viscometer configuration and operation

The overall configuration of the parallel-disk viscometer used in this study is described in the paper (Hirayama et al., 2020). The sliding part of the viscometer consists of an upper specimen and a lower disk, as shown in Figure 1, and the viscometer’s main dimensions are shown in Table 1. The upper specimen is made of stainless steel (SUS440C), and the lower disk is made of borosilicate crown glass (BK7). A surface-restricted aerostatic bearing is located at the center of the upper specimen. An air supply hole is made in the center of the upper specimen, through which compressed air flows to form the aerostatic bearing with the lower disk. The aerostatic bearing face is grooved by etching as the surface restriction that changes the pressure distribution when the gap between the upper specimen and the lower disk changes and can keep the gap constant, owing to the generation of bearing stiffness. The details of the pressure distribution that occurs in aerostatic bearings are explained in the previous paper (Hirayama et al., 2020). The compressed air flows from the center of the upper specimen into the aerostatic bearing area. It is exhausted out of the side of the upper specimen through the deep groove between the aerostatic bearing area and the outer ring area. The lubricating oil or sample grease is sandwiched only in the outer ring area between the upper specimen and the lower disk. The lower disk holder, which does not rotate but is softly supported by the leaf springs, can maintain a parallel between the upper specimen and the lower disk due to the tilting stiffness of the aerostatic bearing. When the upper specimen is rotated by a motor using a belt, an arm attached to the lower disk holder pushes a load cell in the rotating direction, which can measure the shear force of the sample oil or grease in the narrow gap. The rotational force

measured by the load cell for the rotational direction pushed by the arm is represented as F_{rot} , and the total shear force generated in the outer ring area calculated from F_{rot} is represented as F_0 , as shown in Figure 2.

The gap length is changed by varying the pushing load using an air cylinder assembled below the lower disk holder. The pushing load is then measured by a load cell for the vertical direction set between the lower disk holder and the load cell.

2.2 Estimation method for gap length

Here, the method for estimating the gap length in the parallel-disk viscometer is described. When the upper specimen is rotated, the sample oil or grease that is sandwiched between the upper specimen and the lower disk generates the rotational force F_{rot} due to its viscosity. To determine the gap length h by the pushing force using the air cylinder, lubricating oil was used, and the gap length was estimated from the shear force F_0 generated by the lubricating oil sandwiched in the outer ring area. As shown in general tribology studies, the Reynolds number is extremely small because the gap is very narrow. Therefore, the oil flow can be assumed to be laminar, and Newton’s viscosity law can be applied; the rotational torque T_r generated by the shear force of the lubricating oil can be expressed using Eq. 1.

$$T_r = \iint \eta \frac{U(r)}{h} r \cdot r d\theta dr = \iint \eta \frac{r\omega}{h} r \cdot r d\theta dr, \quad (1)$$

where r and θ are arbitrary radius and angle, respectively, η is the known viscosity of the lubricating oil, ω is the angular rotational speed, and h is the gap length. When the inner and outer radii of the outer ring area are represented as r_0 and r_1 , respectively, the integral area for the shear force is $r_0 \leq r \leq r_1$ and $0 \leq \theta \leq 2\pi$. Therefore, the

TABLE 1 Dimensions of the main parts of the parallel-disk viscometer.

Upper specimen		
Material	SUS440C	
Number of grooves		8
Groove area ratio	ψ	0.333 (15° × 8/360°)
Groove radius	r_g [mm] = $d_g/2$	10
Inner hole radius	r_s [mm] = $d_s/2$	1
Bearing outer diameter	r_a [mm] = $d_a/2$	11
Outer ring area inner diameter	r_0 [mm] = $d_0/2$	12
Outer ring area outer diameter	r_1 [mm] = $d_1/2$	15
Bearing area depth	δ [μm]	5
Lower disk		
Product name	OPB-40S04-10-5, SIGMA KOKI	
Material	BK7	
Size	[mm]	40 × 40
Thickness	[mm]	4
Peak to valley	λ/10	
Apparatus		
Rotational speed	[rpm]	0–160
Length of arm	L [mm]	52

rotational torque T_r is defined in Eq. 2. Then, the total shear force F_0 is expressed using Eq. 3.

$$T_r = \int_0^{2\pi} \int_{r_0}^{r_1} \frac{r^3 \omega}{h} \eta \, dr d\theta = \frac{2\pi\omega\eta}{h} \frac{r_1^4 - r_0^4}{4}, \tag{2}$$

$$F_0 = \iint \eta \frac{U(r)}{h} \cdot r \, dr d\theta = \iint \eta \frac{r\omega}{h} r \, dr d\theta = \int_0^{2\pi} \int_{r_0}^{r_1} \frac{r^2 \omega}{h} \eta \, dr d\theta = \frac{2\pi\omega\eta}{h} \frac{r_1^3 - r_0^3}{3}. \tag{3}$$

So, the relationship between the rotational torque T_r and the shear force F_0 generated in the outer ring area can be expressed using Eq. 4.

$$T_r = \frac{3}{4} \frac{r_1^4 - r_0^4}{r_1^3 - r_0^3} \cdot F_0. \tag{4}$$

On the other hand, considering the relationship between the rotational force measured by the load cell located a distance L away from the center of rotation and the rotational torque T_r , it can be expressed as

$$T_r = F_{rot} \cdot L. \tag{5}$$

Therefore, the shear force F_0 required for the gap length estimation can be obtained from the rotational force F_{rot} by

$$F_0 = \frac{4(r_1^3 - r_0^3)}{3(r_1^4 - r_0^4)} \cdot L \cdot F_{rot}. \tag{6}$$

To estimate the gap length h , by differentiating Eq. 3 with respect to the angular velocity ω , the following equation can be derived:

$$h = 2\pi \cdot \frac{r_1^3 - r_0^3}{3} \cdot \eta \cdot \frac{1}{\left(\frac{dT_r}{d\omega}\right)}. \tag{7}$$

Since the inner and outer radii of the upper specimen, r_0 and r_1 , and the viscosity of the base oil, η , are known values, the gap can be estimated by measuring the shear force at each rotational speed.

2.3 Gap length estimation using a base oil

To estimate the gap length h by the pushing force of the air cylinder, three kinds of alkyl diphenyl ether (ADE)-type base oils with different known viscosities were selected. The physical properties of the base oils used are shown in Table 2. The number in the name of each base oil corresponds to the kinematic viscosity at 40°C. Note that ADE is a typical base oil often used as a component of sample greases. The room temperature was maintained at 22°C–23°C in this study.

As an example, Figure 3 shows the rotational force F_{rot} measured by the load cell. The rotational speed of the upper specimen was first rotated at 27 rpm for 20 s, then at 140 rpm for 2 min, and then changed stepwise from 6 to 140 rpm every 15 s. In this experiment, the air pressure on the aerostatic bearing was set constant at 0.3 MPa. In Figure 3, the purple line shows the rotational speed, and the measured F_{rot} values are shown in color. In this example, ADE32 was used. The legend in the figure indicates the pushing force applied by the air cylinder; the larger the pushing

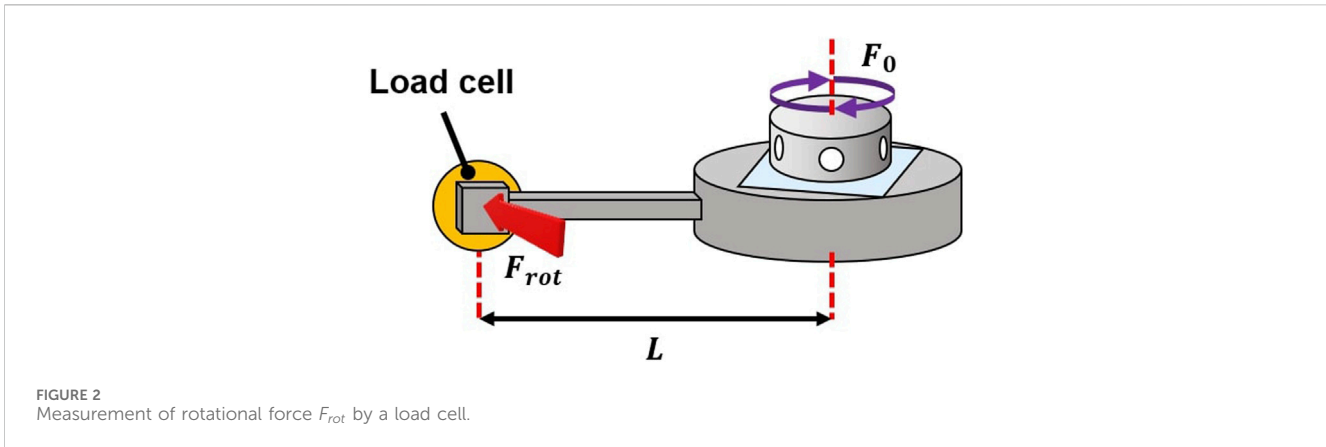


FIGURE 2 Measurement of rotational force F_{rot} by a load cell.

TABLE 2 Kinetic viscosity and viscosity of base oils.

Name	Kinetic viscosity [mm/s] at 40°C	Viscosity [Pa · s] at 25°C
ADE15	15	0.0297
ADE32	32	0.0607
ADE68	68	0.1381

force, the narrower the gap is expected to be. The rotational force F_{rot} was measured stably in all experiments.

To determine the gap length using the pushing force of the air cylinder, the same experiment shown in Figure 3 was conducted with the three base oils listed in Table 2, and F_{rot} for each rotational speed was obtained experimentally. Then, the air pressure to the aerostatic bearing was set at 0.3 MPa, and the pushing forces were set at 40.5, 53.5, and 70.5 N. The shear force F_0 was obtained from F_{rot} in Eq. 6, and the gap length for each rotational speed was calculated using Eq. 7. The estimated gap length for each pushing force is shown in Figure 4. The gap narrowed as the pushing force increased. In addition, it could be confirmed that the gap length did not depend on the rotational speed or the oil viscosity, as confirmed in the previous paper (Hirayama et al., 2020). This proves that it is the balance between the force generated by the aerostatic bearing and the pushing load from the air cylinder that determines the gap length. These preliminary experiments showed that the averaged gap lengths corresponding to the pushing forces of 40.5, 53.5, and 70.5 N are approximately 10, 6, and 3 μm , respectively. It was assumed that this gap length h would also apply to grease as the target sample. Therefore, in the graphs that follow, the experimental results are expressed in terms of the gap length, not the pushing force.

2.4 Calculation of the apparent viscosity of grease

After the gap length h was estimated using the lubricating base oil, the sample grease was sandwiched instead of the lubricating base oil in the outer ring area, and its shear force was measured at each rotational speed. Since the experiment in Section 2.3 has proven that the gap length is constant regardless of the sample viscosity and the

rotational speed of the upper specimen and that the gap length h was estimated at 10, 6, and 3 μm under the pushing forces of 40.5, 53.5, and 70.5 N, respectively, the estimated gap length was newly defined as the known value C_{r_0} . Replacing the gap length h in Eq. 3 with the known gap length C_{r_0} , the viscosity of grease can be defined as follows:

$$\eta = \frac{F_0}{2\pi\omega} C_{r_0} \frac{3}{r_1^3 - r_0^3}. \tag{8}$$

The viscosity η calculated using Eq. 8 is called the apparent viscosity in this study. The equivalent shear rate $\dot{\gamma}$ acting on the grease sandwiched in the gap can be expressed as follows:

$$\dot{\gamma} = \frac{3(r_1^4 - r_0^4)}{4(r_1^3 - r_0^3)} \frac{\omega}{C_{r_0}}. \tag{9}$$

3 Apparent viscosities of greases in the narrow gap at the steady shear rate condition

3.1 Test greases

In this experiment, typical urea grease and lithium grease were used as test greases. Their compositions and physical properties are shown in Table 3. The chemical structures and scanning electron microscopic (SEM) images are shown in Figure 5. Eventually, these samples are denoted as “urea” and “lithium.” The lithium grease used in this experiment is thickened using lithium stearate, which has a chain-like end group, while the urea grease is thickened using aromatic urea, which has a cyclic end group. The difference in the chemical structure of each thickener shown in Figure 5 indicates that the urea grease has a lumpy mesh structure, whereas the lithium grease is intertwined in a fiber-like structure, as shown in the SEM image.

3.2 Experimental procedure

In this study, the viscosity of sample greases was measured at a steady shear rate using a parallel-disk viscometer with a narrow gap. Then, the gap length between the upper specimen and the lower

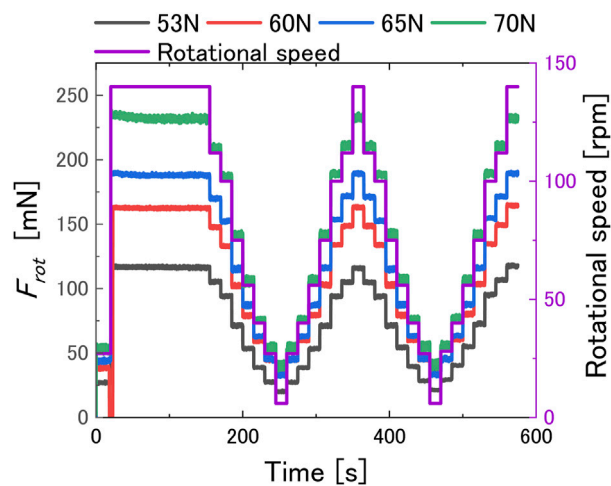


FIGURE 3
Rotational force for the base oil measured at each rotational speed and pushing load.

disk was varied by changing the pushing load, and the relationship between the pushing load and the gap length is determined in Section 2.3. The experimental procedure is described as follows:

1. Start rotating the upper specimen at 40 rpm for 20 s to distribute grease over the sliding surface.
2. Start rotating the upper specimen at 160 rpm, the maximum speed, for 600 s. This operation allows the grease to be homogeneously placed in the gap and the stable shear force to be measured.
3. Measure the shear force while decelerating every 60 s from the maximum speed of 160 rpm to a minimum speed of 20 rpm. The set of rotational speeds was [160, 140, 120, 100, 80, 60, 40, and 20] rpm.
4. Measure the shear force while accelerating every 60 s from 20 rpm to the maximum speed of 160 rpm after the rotational speed reaches 20 rpm. The set of rotational speeds was the same as shown in the previous step but in reverse order.
5. Stop the rotation and finish the experiment.

3.3 Experimental results and discussion

Figure 6 shows the rotational force F_{rot} measured by the load cell when rotating the upper specimen by sandwiching the sample grease in the narrow gap. Similar to the behavior of the base oil, a narrower gap length resulted in a higher F_{rot} value. In contrast to Figure 3, which is the result of the experiment with the base oil, Figure 6 shows a characteristic delayed response when the rotational speed decelerates in a stepwise manner. This characteristic delayed response was significantly observed as the gap became narrower. When calculating the apparent viscosity of the grease at each sliding speed, the average value of the last 4 s of each rotation process was used as F_{rot} , and the apparent viscosity was calculated using Eqs 6, 8.

Figure 7 shows the apparent viscosity of each grease at gaps 10, 6, and 3 μm , where the horizontal axis is the shear rate, which is calculated using Eq. 9. In the figure, the viscosity measured using a commercial rheometer with parallel plates (Physcia MCR 301,

Anton Paar) is also shown. In the measurement, the gap lengths between the plates were set at 150, 350, and 700 μm , and the shear rate was calculated at the outer diameter of the plate at $\phi 25$ mm. The temperature setting was set at 23°C to be consistent with the room temperature in the laboratory. Figure 7 shows that the apparent viscosity of the grease decreased with the increasing shear rate regardless of the grease type and gap length, so-called ‘shear thinning’ behavior. However, the apparent viscosities of both greases measured in the narrow gap were lower than those measured in the sufficiently wide gap. Furthermore, this trend was more pronounced for narrower gap lengths. Shear properties at this narrow gap are described in more detail.

At a shear rate of approximately $10,000 \text{ s}^{-1}$, as shown in Figure 7, the trend in apparent viscosity changes near that point. Below $10,000 \text{ s}^{-1}$, the apparent viscosity remains almost constant, independent of the shear rate. On the other hand, above $10,000 \text{ s}^{-1}$, the apparent viscosity decreases as the shear rate increases. The apparent viscosity in the former range is clearly lower than that measured using the commercial viscometer with a submillimeter gap. This trend can therefore be attributed to the narrow gap in the micrometer order. General shear thinning is due to the orientation of the internal structure of the material as the shear rate increases, and the shear force then decreases. However, at this low shear rate range below $10,000 \text{ s}^{-1}$, the apparent viscosity is almost constant, and there does not appear to be a progression in the orientation of the grease thickener dependent on the shear rate. This can be attributed to the fact that the thickener is already oriented by being forced into a narrow gap. On the other hand, at the high shear rate range above $10,000 \text{ s}^{-1}$, the so-called shear thinning property is considered to be due to the further orientation of the thickening in grease as a result of the high shear force applied. The fact that the apparent viscosity curve in the high shear rate range measured in a narrow gap is almost an extension of the apparent viscosity curve measured in a millimeter-order gap also supports the argument. It can thus be said that there are two types of thickener orientation mechanisms, which can be relatively clearly demarcated: one is the orientation produced by a narrow gap, and the other is the orientation driven by shear force.

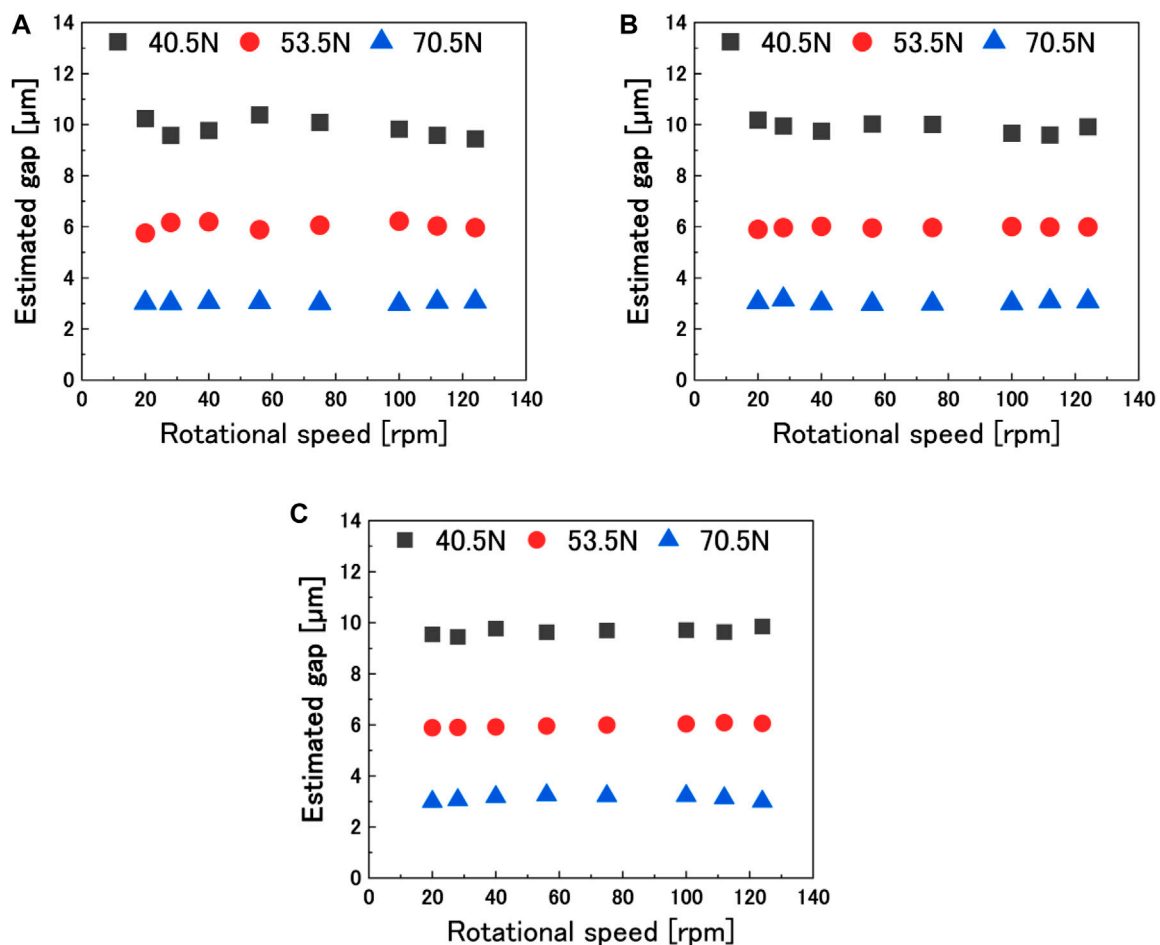


FIGURE 4
Estimated gap using the base oil under several pushing loads: (A) ADE15, (B) ADE32, and (C) ADE68.

There have been many studies on the orientation of grease thickeners from the past, but most of them are due to shear forces. For example, Hokao et al. investigated the morphology of shear-induced structural changes in the thickener and reported that the higher the shear force, the clearer the orientation of the thickener fibers (Hokao et al., 2019). However, no study has been found when the gap length is equivalent to the size of grease thickeners, and it can be said that this study could propose a novel mechanism for the viscosity behaviors of greases in an environment close to the actual tribological field.

4 Viscoelastic behaviors of greases in narrow gaps with changing speed conditions

4.1 Experimental procedure

As mentioned earlier, when the rotational speed changed, F_{rot} of the urea grease in Figure 6 showed a delayed response that was not found in the results for the base oil shown in Figure 3; therefore, this delayed response is a grease-specific behavior. To investigate whether this delayed response depends on the gap length and

grease type, the shear force behavior was investigated when the rotational speed of the upper specimen was instantaneously changed as a step input under constant gap conditions. The upper specimen and the lower disk are identical to those used above. The experimental procedure is as follows:

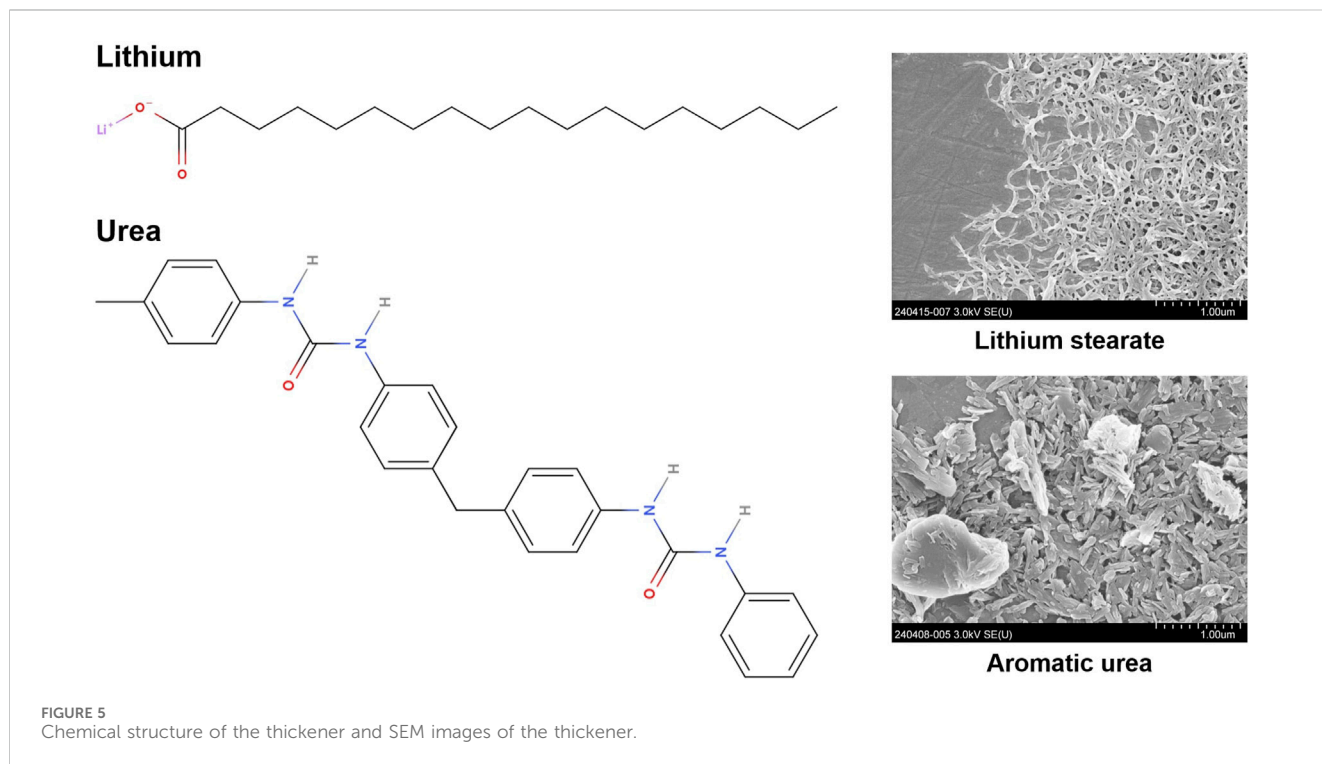
1. Start rotating the upper specimen at 160 rpm, the maximum speed, for 600 s. This operation allows the grease to be homogeneously placed in the gap and ensures stable measurement of shear force.
2. Set the pushing load to 50, 60, and 68 N, respectively, and rotate the motor at 40 rpm for 5 min. Then, change the rotational speed instantaneously to 160 rpm as a step input and maintain the speed for 5 min. Measure the shear force continuously during this procedure.
3. Stop the rotation and finish the experiment.

4.2 Experimental results

The experimental results for F_{rot} of the base oil, urea grease, and lithium grease are shown in Figure 8. As described above, with the base oil, there was no delay in response when the rotational speed

TABLE 3 Composition and properties of sample greases (Komiya et al., 2019).

Sample name	Urea	Lithium
Base oil	Alkyl diphenyl ether (ADE)	
Material of the thickener	Aromatic urea	Lithium stearate
Thickener concentration mass%	20.7	13.3
Kinematic viscosity of base oil (40°C), mm ² /s	101.7	
Worked penetration @ 60W	269	251



was changed as a step input, but there were characteristic delayed responses for both cases with the urea and lithium greases. In the previous chapter, it was mentioned that the gap length has a significant effect on the shear response of the grease, which promotes the orientation of the thickener, and this delayed response can also be attributed to the orientation behavior of the thickener. This delayed response was more marked as the gap became narrower. Since the micrometer-order gap length promotes thickener orientation, a quantitative evaluation of this delayed response was determined using the relaxation time.

For example, in stress relaxation tests, when the initial stress is σ_0 , the change in stress with time can be expressed, as shown in Eq. 10, where G and η are the elastic modulus and viscosity, respectively.

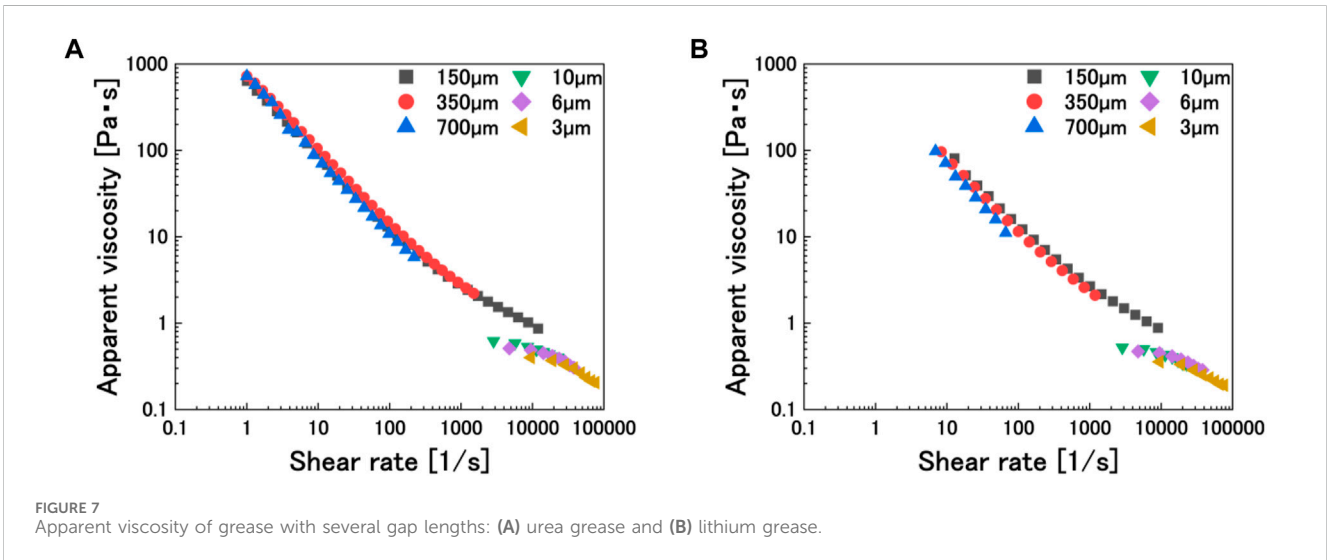
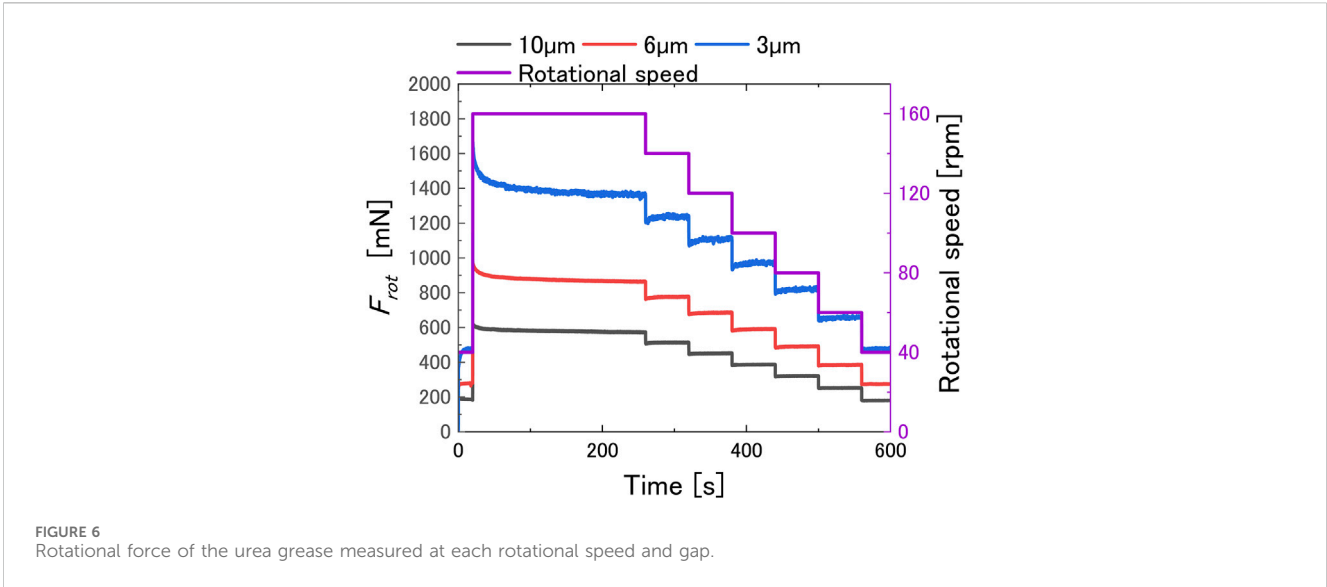
$$\sigma(t) = \sigma_0 \left\{ \exp\left(-\frac{t}{\tau}\right) \right\}, \quad \tau = \frac{\eta}{G}. \quad (10)$$

The relaxation time τ is defined as $\tau = \eta/G$, indicating the time required for the stress to reach $1/e$ of the initial value σ_0 , representing the speed of relaxation. Generally, the relaxation time τ is used as the time required to reach approximately 63%

of the equilibrium state, but in this experiment, it was defined as the time required to reach 90% of the convergence value because of the concern that the time required to reach 63% of the convergence value was too short and would result in large errors. Curve fitting was performed for the obtained F_{rot} curves by smoothing the data using a moving average method starting from the peak point of F_{rot} after the rotation speed was instantaneously changed from 40 rpm to 160 rpm. If the number of data points to be smoothed is k , the value to be smoothed is x_t , and the smoothed value is MA_t . Eq. 11 represents the formula for the moving average method. The sampling frequency in this experiment was 100 Hz, and the measurement time increment for one cell was 10 m and $k = 150$. Curve fitting on the smoothed data resulted in $R^2 \geq 0.985$ for all fittings.

$$MA_t = \frac{1}{k} \sum_{i=1}^k x_{t-i+1}. \quad (11)$$

The relationship between the relaxation time τ and the pushing load for each grease obtained from the fitting curves is shown in Figure 9. The gap lengths corresponding to each pushing load are



indicated by dotted lines in the graph. For both urea grease and lithium grease, the relaxation time τ increased as the pushing load increased, i.e., as the gap narrowed. The increase in relaxation time indicates that it takes a longer time to stabilize after the instantaneous changes in the share rate as the gap length narrows. The pushing load and relaxation time showed a good correlation, and the slope of the linear approximation of the relaxation time was higher for the lithium grease than for the urea grease. This result may be attributed to the difference in the thickener structure within the grease.

4.3 Discussion

First, we need to address the possibility that the viscosity of the sample has changed due to the high shear rate of the sample in the narrow gap. However, because the oil film is airtight and thin, it is

difficult to control or measure temperature directly. Of course, heat is generated by sliding, but the heat generated is transferred quickly to the upper specimen and the lower disk due to their large heat capacities; therefore, the viscosity of the sample oil barely changes. The evidence suggests that Figure 3 shows that F_{rot} did not change under constant rotational speed. If the viscosity of the sample changed due to the generated heat, the value of F_{rot} should decrease gradually, even at a constant shear rate. However, at the same shear rate, F_{rot} was the same in all regions, so a change in the viscosity of the sample due to temperature change is not expected. When measuring the gap using the base oil, the amount of heat generated by the shear should be changed in accordance with the shear rates. Still, since a constant gap length was obtained regardless of the shear rate, the viscosity change by heat is not considered to affect this measurement. The same explanation can be applied to the grease shown in Figure 6. If the viscosity of the grease decreases due to the temperature increase, F_{rot} should decrease gradually under

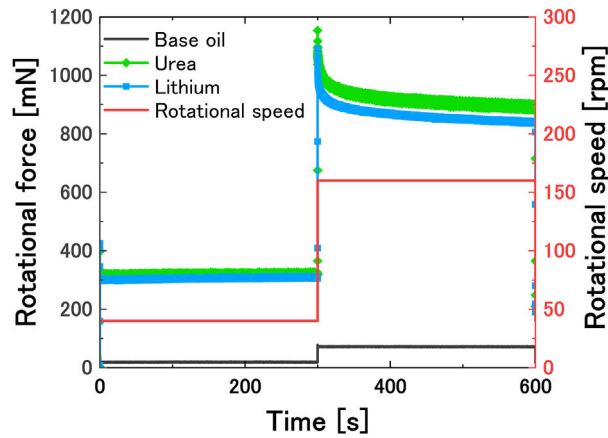


FIGURE 8 Relaxation behaviors of base oil, urea grease, and lithium grease for the step input of rotational speed.

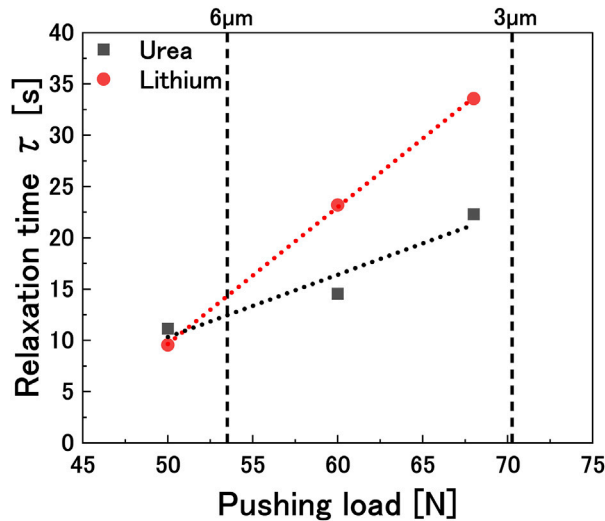


FIGURE 9 90% relaxation time of each grease according to the pushing load.

constant shear. The temperature increase due to sliding was a point of concern for us as well, but the temperature after the test matched that before the experiment by one decimal digit. Therefore, we believe that no significant temperature increase occurred that would change the viscosity.

As shown in Figure 9, the relaxation time of the grease increased linearly with increasing the pushing load, i.e., with decreasing gap length. In the experiment, the rotation speed of the upper specimen was changed as a step input from 40 to 160 rpm, and the rate of change of the shear rate in the gap is also greater when the gap is narrower. Therefore, it takes time for the grease to orient itself in response to the change in the shear rate, so the relaxation time was longer when the gap was narrower.

On the other hand, Figure 9 shows that the relaxation time increased with the decreasing gap for the lithium stearate grease compared to the aromatic urea grease. This means that the urea

grease stabilized faster when subjected to the same change in the shear rate. Since this difference could be attributed to the type of thickener, it was discussed in connection with the ‘grease film-forming ability’ of each grease. The ‘grease film-forming ability’ is a technical term used to describe the ease of forming a grease film to separate the contact surfaces and the strength of the formed grease film; the higher the grease film-forming ability, the easier it is for the contact surfaces to remain non-contact. Komiya et al. (2019) used five types of greases with different thickeners, including the aromatic urea grease and lithium stearate grease used in our study, and examined the grease film-forming ability of each grease using a two-cylinder tester. They measured the contact ratio between the two cylinders using an electric potential difference method when grease was supplied between the two cylinders and rotated in a pure rolling condition. The value calculated from

the contact ratio was called the ‘grease film-forming rate,’ with 0% defined as a complete contact state, 100% as a complete non-contact state, and values in between as partial contact states. As a result, with the lithium grease, the grease film-forming rate between the two cylinders gradually increased as the rotation speed increased, reaching a maximum of 80%, but the grease film-forming rate remained at almost 80% even at the highest rotation speed. On the other hand, the urea grease reached a grease film-forming rate of 80% immediately after the start of the test, even at low speeds, and maintained 100% grease film formation at higher speeds. The tendency of the relaxation time of the lithium grease to be longer than that of the urea grease, as shown in Figure 9, is considered to correlate with this grease film-forming ability. When the shear rate changes, the aromatic urea grease immediately forms a stable grease film due to the entanglement of aromatic rings in the thickener, whereas the lithium stearate grease takes longer to form a stable grease film due to less entanglement of thickeners. The longer relaxation time of the lithium grease, as shown in Figure 9, is considered to be due to this same phenomenon occurring in the grease film.

In addition, it can be explained by the structural complexity of the thickener. Xu et al. investigated the structure strength, structural rearrangement speed, and recoverability of several lithium greases. As a result, the higher the entanglement level of the thickener, the higher the structure strength, the slower the rearrangement speed, and the lower the recoverability of the grease (Xu et al., 2018). Considering urea and lithium used in this experiment, lithium, which has a long mesh structure, seems to have a higher entanglement level than urea, which has independent clumps of short fibers, as shown in Figure 5. It is believed that the high entanglement required more time for the thickener to reorient, resulting in a longer relaxation time, similar to the experiment conducted by Xu et al.

As described in Section 4.1, the time-dependent curves that appear when the rotational speed is changed are attributed to the thickener microstructure, which requires time for reorientation in response to changes in the shear rate. The mechanism of the characteristic curves that appear in Figures 6, 8 during deceleration and acceleration will be discussed, concerning the degree of orientation of the thickener. Consider the case of deceleration, i.e., when the shear force exerted on the grease is reduced. Before deceleration, the thickener is considered to be strongly oriented in the shear direction due to the high shear force. When the shear rate is rapidly decreased from this state, the thickener is subjected to a low shear force while maintaining a high degree of orientation, so F_{rot} , which indicates the viscous resistance of the grease, is temporarily and significantly dropped. Then, as time passes, the thickener gradually loses its high orientation and F_{rot} increases. Eventually, as time progresses, the reorientation of the thickener is complete and becomes stable, and F_{rot} reaches a constant value. On the other hand, considering the mechanism of acceleration, before acceleration, the thickener is slightly oriented in the shear direction by the shear force. When the shear rate increases from this state, the thickener, which has a low orientation in the shear direction, is subjected to a high

shear force. Therefore, the viscous resistance increases rapidly, and the F_{rot} value increases significantly. The thickener is gradually more oriented by the high shear force, and F_{rot} gradually decreases. Similar to the deceleration, the structure of the thickener stabilizes over time, and F_{rot} becomes a constant value. As described above, the curve that appears when shear is changed is thought to be due to the reorientation of the thickener structure, which takes time.

5 Conclusion

In this study, the apparent viscosity and the shear force behavior of urea and lithium greases in the micrometer-order gap were investigated using the parallel-disk viscometer. The conclusions drawn from this study are as follows:

- The apparent viscosity of the urea grease and lithium grease decreased as the gap became narrower under shear rates below $10,000 \text{ s}^{-1}$. This is thought to be due to shear thinning caused by the grease being pressed down by the narrow gap. On the other hand, the orientation of the thickener due to the high shear rate was observed in the range of $10,000 \text{ s}^{-1}$ or higher. Thus, two types of shear thinning mechanisms were proposed for thickener orientation: one caused by a narrow gap and the other by the shear force.
- When the grease was subjected to shear change, a characteristic curve appeared. The curve was caused by the fact that it takes time for the thickener structure to reorient in response to the shear force that changed, which showed the reorientation mechanism of the thickener during acceleration and deceleration. The time requirement was quantitatively evaluated in terms of relaxation time, and it was shown that the relaxation time increases as the gap narrows, and the degree of increase depends on the thickener and is correlated with the oil film-forming ability of the grease and the entanglement level of the thickener.

Data availability statement

The original contributions presented in the study are included in the article/Supplementary Material; further inquiries can be directed to the corresponding author.

Author contributions

HC: data curation, formal analysis, methodology, writing—original draft, writing—review and editing, investigation, and visualization. TH: conceptualization, software, supervision, and writing—review and editing. NY: writing—review and editing, supervision, and validation. NH: software and writing—review and editing. KT: resources and writing—review and editing. RK: resources and writing—review and editing.

Funding

The authors declare that no financial support was received for the research, authorship, and/or publication of this article.

Acknowledgments

The authors would like to thank all the people who assisted in the conduct of this study. The base oil and grease samples were provided by MORESCO Corporation and Nippon Grease Co., Ltd., respectively. They would also like to thank Mr. Heegwan Son for his helpful advice on building a data analysis program.

References

- Abdali, S. S., Mitsoulis, E., and Markatos, N. C. (1992). Entry and exit flows of Bingham fluids. *J. Rheol. (N Y N Y)* 36, 389–407. doi:10.1122/1.550350
- Akhtar, K., Khalid, H., Ul Haq, I., and Malik, A. (2016). Improvement in tribological properties of lubricating grease with quartz-enriched rice husk ash. *Tribol. Int.* 93, 58–62. doi:10.1016/j.triboint.2015.09.015
- Bhushan, B., and Ko, P. (2003). Introduction to tribology. *Appl. Mech. Rev.* 56, B6–B7. doi:10.1115/1.1523360
- Bristeau, M. O., Glowinski, R., Mantel, B., Periaux, J., Perrier, P., and Pironneau, O. (1980). "A finite element approximation of Navier-Stokes equations for incompressible viscous fluids. Iterative methods of solution," in *Approximation methods for Navier-Stokes problems*. Editor R. Rautmann (Berlin, Heidelberg: Springer Berlin Heidelberg), 78–128. doi:10.1007/BFb0086902
- Bukvić, M., Gajević, S., Skulić, A., Savić, S., Ašonja, A., and Stojanović, B. (2024). Tribological application of nanocomposite additives in industrial oils. *Lubricants* 12, 6. doi:10.3390/lubricants12010006
- Camousseigt, L., Galfré, A., Couenne, F., Oumahi, C., Muller, S., and Tayakout-Fayolle, M. (2023). Oil-bleeding dynamic model to predict permeability characteristics of lubricating grease. *Tribol. Int.* 183, 108418. doi:10.1016/j.triboint.2023.108418
- Cann, P., and Lubrecht, A. A. (1999). An analysis of the mechanisms of grease lubrication in rolling element bearings. *Lubr. Sci.* 11, 227–245. doi:10.1002/ls.3010110303
- Cann, P. M. (2007). Grease lubrication of rolling element bearings — role of the grease thickener. *Lubr. Sci.* 19, 183–196. doi:10.1002/ls.39
- Cann, P. M., Doner, J. P., Webster, M. N., and Wikstrom, V. (2001). Grease degradation in rolling element bearings. *Tribol. Trans.* 44, 399–404. doi:10.1080/10402000108982473
- Cen, H., and Lugt, P. M. (2019). Film thickness in a grease lubricated ball bearing. *Tribol. Int.* 134, 26–35. doi:10.1016/j.triboint.2019.01.032
- Chapkov, A. D., Bair, S., Cann, P., and Lubrecht, A. A. (2007). Film thickness in point contacts under generalized Newtonian EHL conditions: numerical and experimental analysis. *Tribol. Int.* 40, 1474–1478. doi:10.1016/j.triboint.2007.01.002
- Chatra, K. R. S., and Lugt, P. M. (2020). Channeling behavior of lubricating greases in rolling bearings: identification and characterization. *Tribol. Int.* 143, 106061. doi:10.1016/j.triboint.2019.106061
- Chatra, K. R. S., and Lugt, P. M. (2021). The process of churning in a grease lubricated rolling bearing: channeling and clearing. *Tribol. Int.* 153, 106661. doi:10.1016/j.triboint.2020.106661
- Chatra, K. R. S., Osara, J. A., and Lugt, P. M. (2022). Impact of grease churning on grease leakage, oil bleeding and grease rheology. *Tribol. Int.* 176, 107926. doi:10.1016/j.triboint.2022.107926
- Cousseau, T., Graça, B., Campos, A., and Seabra, J. (2011). Friction torque in grease lubricated thrust ball bearings. *Tribol. Int.* 44, 523–531. doi:10.1016/j.triboint.2010.06.013
- Delgado, M. A., Sánchez, M. C., Valencia, C., Franco, J. M., and Gallegos, C. (2005). Relationship among microstructure, rheology and processing of a lithium lubricating grease. *Chem. Eng. Res. Des.* 83, 1085–1092. doi:10.1205/cherd.04311
- Farfan-Cabrera, L. I. (2019). Tribology of electric vehicles: a review of critical components, current state and future improvement trends. *Tribol. Int.* 138, 473–486. doi:10.1016/j.triboint.2019.06.029
- Gao, W., Nelas, D., Boisson, N., and Lyu, Y. (2018). Model formulation of churning losses in cylindrical roller bearings based on numerical simulation. *Tribol. Int.* 121, 420–434. doi:10.1016/j.triboint.2018.02.003

Conflict of interest

The authors declare that the research was conducted in the absence of any commercial or financial relationships that could be construed as a potential conflict of interest.

Publisher's note

All claims expressed in this article are solely those of the authors and do not necessarily represent those of their affiliated organizations, or those of the publisher, the editors, and the reviewers. Any product that may be evaluated in this article, or claim that may be made by its manufacturer, is not guaranteed or endorsed by the publisher.

- Gohar, R., and Rahnejat, H. (2018). Fundamentals of tribology. *World Sci.*
- Hirayama, T., Shibata, S., Harada, T., Hashimoto, Y., and Yamashita, N. (2020). Shear property of oil film containing oiliness additive in narrow gap measured with newly-developed parallel-disk viscometer supported by aerostatic bearing. *Lubr. Sci.* 32, 46–57. doi:10.1002/ls.1485
- Hokao, M., Sonoda, K., and Sugimura, J. (2019). The relationship between structural change of thickeners and rheological properties on lubricating grease. *J. Jpn. Soc. Tribol.* 64, 42–54. doi:10.18914/tribologist.18-00017
- Hotten, B. W. (1955). Optical studies of lubricating grease structure. *NLGI Spokesm.* 19, 14.
- Hutton, J. F. (1975). "The influence of flow elasticity on the bearing performance of lubricating greases," in Proc JSLE-ASLE International Lubrication Conference, ASLE, July 1, 1976, 707–714.
- Kandeva, M., Karastoyanov, D., Assenova, E., Jakimovska, K., Simeonov, S., and Vencel, A. (2016). The influence of the valena metal-plating additive on tribotechnical characteristics of the Steel–Bronze tribological system. *J. Frict. Wear* 37, 187–190. doi:10.3103/S1068366616020082
- Komiya, H., Geshi, Y., Yaotani, N., Hirayama, T., Matsuoka, T., and Sakamoto, H. (2019). Effects of thickener on oil film formation of lubricating grease: mechanism of grease film formation with adhesion/deposition of thickener on friction surface. *J. Jpn. Soc. Tribol.* 64, 33–41. doi:10.18914/tribologist.18-00012
- Lugt, P. M. (2009). A review on grease lubrication in rolling bearings. *Tribol. Trans.* 52, 470–480. doi:10.1080/10402000802687940
- Lugt, P. M. (2016). Modern advancements in lubricating grease technology. *Tribol. Int.* 97, 467–477. doi:10.1016/j.triboint.2016.01.045
- Lugt, P. M., Holgersson, M., and Reinholdsson, F. (2023). Impact of oxidation on grease life in rolling bearings. *Tribol. Int.* 188, 108785. doi:10.1016/j.triboint.2023.108785
- Maksimova, Y. M., Shakhmatova, A. S., Ilyin, S. O., Pakhmanova, O. A., Lyadov, A. S., Antonov, S. V., et al. (2018). Rheological and tribological properties of lubricating greases based on esters and polyurea thickeners. *Pet. Chem.* 58, 1064–1069. doi:10.1134/S0965544118120071
- Mansot, J. L., Terech, P., and Martin, J. M. (1989). Structural investigation of lubricating greases. *Colloids Surfaces* 39, 321–333. doi:10.1016/0166-6622(89)80283-5
- Mubashshir, M., and Shaikat, A. (2019). The role of grease composition and rheology in elastohydrodynamic lubrication. *Tribol. Lett.* 67, 104. doi:10.1007/s11249-019-1218-z
- Noda, T., Shibasaki, K., Miyata, S., and Taniguchi, M. (2020). X-ray CT imaging of grease behavior in ball bearing and numerical validation of multi-phase flows simulation. *Tribol. Online* 15, 36–44. doi:10.2474/trol.15.36
- Obata, T., Fujiwara, H., Itoigawa, F., and Maegawa, S. (2024). Effect of grease viscosity on channeling properties of ball bearings. *Lubricants* 12, 13. doi:10.3390/lubricants12010013
- Onoda, E., Nogi, T., and Moriuchi, T. (2021). Observation technologies for grease thickener. *J. Jpn. Soc. Tribol.* 66, 676–681. doi:10.18914/tribologist.66.09_676
- Radulescu, A. V., Bonneau, D., and Hajjam, M. (2003). A theoretical study of two-dimensional grease flow in regions with discontinuities. *Lubr. Sci.* 15, 163–171. doi:10.1002/ls.3010150206
- Rawat, S. S., and Harsha, A. P. (2019). "Current and future trends in grease lubrication," in *Automotive tribology*. Editors J. K. Katiyar, S. Bhattacharya, V. K. Patel, and V. Kumar (Singapore: Springer Singapore), 147–182. doi:10.1007/978-981-15-0434-1_9

- Saatchi, A., Shiller, P. J., Egtesadi, S. A., Liu, T., and Doll, G. L. (2017). A fundamental study of oil release mechanism in soap and non-soap thickened greases. *Tribol. Int.* 110, 333–340. doi:10.1016/j.triboint.2017.02.004
- Sakai, K., Ayame, Y., Iwanami, Y., Kimura, N., and Matsumoto, Y. (2021). Observation of grease fluidity in a ball bearing using neutron imaging technology. *Tribol. Online* 16, 146–150. doi:10.2474/TROL.16.146
- Shah, R., Tung, S., Chen, R., and Miller, R. (2021). Grease performance requirements and future perspectives for electric and hybrid vehicle applications. *Lubricants* 9, 40. doi:10.3390/lubricants9040040
- Shetty, P., Meijer, R. J., Osara, J. A., Pasaribu, R., and Lugt, P. M. (2024). Effect of grease filling on the film thickness in deep-groove ball bearings. *Tribol. Trans.* 67, 62–69. doi:10.1080/10402004.2023.2282632
- Suetsugu, Y., Sekiguchi, H., Nakanishi, Y., Fujinami, Y., and Ohno, T. (2013). Basic study of grease rheology and correlation with grease properties. *Tribol. Online* 8, 83–89. doi:10.2474/trol.8.83
- Woydt, M. (2021). The importance of tribology for reducing CO2 emissions and for sustainability. *Wear* 474–475, 203768–204475. doi:10.1016/j.wear.2021.203768
- Wu, M., Han, X., Tao, Y., and Pei, J. (2022). A mixed EHL analysis method for grease and formulas for film thickness and asperity load. *Tribol. Lett.* 70, 128. doi:10.1007/s11249-022-01666-4
- Xu, N., Wang, X., Ma, R., Li, W., and Zhang, M. (2018). Insights into the rheological behaviors and tribological performances of lubricating grease: entangled structure of a fiber thickener and functional groups of a base oil. *New J. Chem.* 42, 1484–1491. doi:10.1039/c7nj04833e